imaging (MRI) of the brain and spinal cord demonstrated normal findings. Gait disturbance and hand tremor gradually improved and the patient was discharged. On day 13, varicella skin lesions appeared and the patient was administered acyclovir (800 mg/day for 5 days). However, gait disturbance and hand tremor worsened on day 14, and the patient was unable to walk on day 16. The child was re-admitted to hospital on day 18. The patient's sister demonstrated apparent parotitis on the same day. CSF examination on day 18 demonstrated pleocytosis (144 mononuclear cells and 6 polynuclear cells/μl), protein 28 mg/dl and glucose 50 mg/dl. The mumps virus was detected in CSF by the polymerase chain reaction (PCR), while the varicella and herpes simplex virus were not. A brain MRI, on day 22, demonstrated normal findings except for meningeal enhancement (Fig. 1). The patient was referred to our hospital on that day. On examination, the child was awake and alert. The patient could sit without assistance but was unable to walk. Mild tremor of the hands and muscular hypotonia were noted. CSF examination, on day 22 of illness, demonstrated 27 mononuclear cells/μl, protein 41 mg/dl, glucose 41 mg/dl, lactate 12.6 mg/dl, pyruvate 0.86 mg/dl, myelin basic protein 45.5 pg/ml and negative oligoclonal band. CSF cytokines were normal except for a mild elevation of interleukin-2 (15.9 pg/ml, normal < 4.6). Autoantibody to GluRδ2 (only IgM without IgG) was positive in serum and CSF. The patient was able to walk with support and was discharged on day 37. On day 60, the patient could walk with a wide-base gait. On the same day, IgM anti-GluRδ2 antibody was weakly positive, however, IgG anti-GluRδ2 antibody remained negative in serum. Anti-varicella and mumps virus IgG antibodies were measured by enzyme-linked immunosorbent assay, showing a more than fourfold rise in antibody titer between day 22 and 60, 500 and 2100 and <230 to 3800, respectively. Six months after the onset, lymphocyte stimulation tests (LST) were conducted using homogenate of D33 (cell line expressing GluRδ2 subunits) [4]. Cell proliferation was measured by ^{3}H-thymidine uptake, and the ratio of the counts of the stimulated samples to the control counts was evaluated as the stimulation index (SI), with an SI > 2 regarded as positive [4,5]. SI with D33 homogenate stimulation was 3.8.

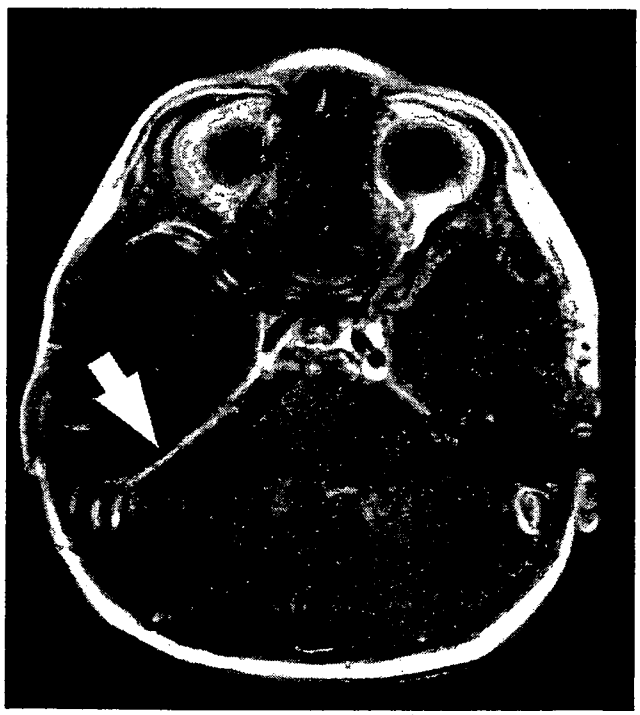

Fig. 1. An axial gadolinium-enhanced T1-weighted MRI, on day 21, shows meningeal enhancement (arrow).

3. Discussion

ACA is diagnosed on clinical grounds with CSF pleocytosis (>5/μl) present in approximately one half of ACA children, ranging from 0 to 107/μl. The absence of neuroimaging abnormalities is not a prerequisite of ACA diagnosis [1,2]. Several authors reported acute ataxic cases with MRI abnormalities, involving the cerebellum and/or brain stem, as ACA [6]. Others reported such cases as acute cerebellitis (AC). Sawaishi et al. reviewed case reports of AC; all had cerebellar lesions, and meningeal enhancement was detected in 3 out of 18 cases and CSF pleocytosis was present in 14 out of 18 cases, ranging from 0 to 1450/μl [7]. However, the distinction between ACA and AC is somewhat obscure; meningeal enhancement could suggest that the re-exacerbation of ataxia observed in this patient was due to consecutive cerebellitis. Thus, the characterization of ACA and AC must be established more precisely.

GluRδ2 is predominantly expressed in cerebellar Purkinje cells [3]. In previous studies, GluRδ2 gene knockout or mutated mice displayed ataxia and injection of the antibody, specific for the ligand-binding region of GluRδ2, into the subarachinoidal supracerebellar space of adult mice caused transient cerebellar dysfunction, including ataxia [3]. Anti-GluRδ2 autoantibody has also been reported in a patient with chronic cerebellitis, showing fluctuation of cerebellar ataxia for 2 years [8]. In that case, anti-GluRδ2 IgM and IgG antibodies were both positive during the first episode of ataxia. In our patient, anti-GluRδ2 IgM antibody was positive not only in plasma but also CSF, and the level decreased with clinical improvement. However, lymphocytes stimulated by LST are usually T cells, thus a positive LST result with homogenate of D33, a cell line expressing GluRδ2 subunits, could comprise T cell activation

[4,5]. We estimated that these GluRδ2 autoantibodies and a positive LST result were produced by cross-reaction as a result of molecular mimicry following viral infection, and played an important role in consecutive cerebellitis in the present case.

To date, there have been several reports of ACA or AC associated with autoantibodies, such as anti-centrosome antibody post-varicella and anti-triosephosphate isomerase antibody after Epstein-Barr viral infection [9,10]. However, these reports did not contain detailed clinical descriptions, thus, it is difficult to say whether there are any clinical differences, including CSF and brain MRI findings, in ACA/AC with or without related autoantibodies. Follow-up of cerebellar ataxia and anti-GluRδ2 autoantibody in our patient could further clarify this relationship. Moreover, humoral or cytological immunologic examinations in ACA/AC patients might clarify their pathogenesis.

Acknowledgment

We thank Dr. Takashi Ichiyama (Department of Pediatrics, Yamaguchi University School of Medicine, Yamaguchi, Japan) for CSF cytokine measurement.

References

[1] Connolly AM, Dodson WE, Prensky AL, Rust RS. Course and outcome of acute cerebellar ataxia. Ann Neurol 1994;35:673–9.
[2] Nussinovitch M, Prais D, Volovitz B, Shapiro R, Amir J. Post-infectious acute cerebellar ataxia in children. Clin Pediatr 2003;42:581–4.
[3] Hirai H, Launey T, Mikawa S, Torashima T, Yanagihara D, Kasaura T, et al. New role of delta 2-glutamate receptors in AMPA receptor trafficking and cerebellar function. Nat Neurosci 2003;6:869–76.
[4] Takahashi Y, Mori H, Mishina M, Watanabe M, Kondo N, Shimomura J, et al. Autoantibodies and cell-mediated autoimmunity to NMDA-type GluRepsilon2 in patients with Rasmussen's encephalitis and chronic progressive epilepsia partialis continua. Epilepsia 2005;46(Suppl.):152–8.
[5] Pichler WJ, Tilch J. The lymphocyte transformation test in the diagnosis of drug hypersensitivity. Allergy 2004;59:809–20.
[6] Maggi G, Varone A, Aliberti F. Acute cerebellar ataxia in children. Childs Nerv Syst 1997;13:542–5.
[7] Sawaishi Y, Takada G. Acute cerebellitis. Cerebellum 2002;1:223–8.
[8] Sugiyama N, Hamano S, Mochizuki M, Tanaka M, Takahashi Y. A case of chronic cerebellitis with anti-glutamate receptor delta 2 antibody (in Japanese). No To Hattatsu (Tokyo) 2004;36:60–3.
[9] Fritzler MJ, Zhang M, Stinton LM, Rattner JB. Spectrum of centrosome autoantibodies in childhood varicella and post-varicella acute cerebellar ataxia. BMC Pediatr 2003;3:11.
[10] Uchibori A, Sakuta M, Kusunoki S, Chiba A. Autoantibodies in postinfectious acute cerebellar ataxia. Neurology 2005;65:1114–6.

ELSEVIER

Brain & Development 29 (2007) 224–226

BRAIN & DEVELOPMENT
Official Journal of the Japanese Society of Child Neurology

www.elsevier.com/locate/braindev

Case report

A case of acute cerebellitis accompanied by autoantibodies against glutamate receptor δ2

Tomoyuki Shimokaze [a,b,*], Mitsuhiro Kato [b], Yozo Yoshimura [a], Yukitoshi Takahashi [c], Kiyoshi Hayasaka [b]

[a] *Department of Pediatrics, Yamagata Prefectural Shinjo Hospital, Shinjo, Japan*
[b] *Department of Pediatrics, Yamagata University School of Medicine, 2-2-2 Iida-nishi, Yamagata city, Yamagata, 990-8545, Japan*
[c] *Department of Pediatrics, National Epilepsy Center, Shizuoka, Japan*

Received 20 July 2006; received in revised form 17 August 2006; accepted 22 August 2006

Abstract

A 13-year-old boy presented with a six-day history of headache and gradually developed severe meningeal irritation symptoms. Brain magnetic resonance imaging revealed left cerebellar swelling and obstructive hydrocephalus. Then he showed transient ataxia, but recovered without any sequelae soon after high dose steroid therapy. IgG type of autoantibodies against glutamate receptor δ2 (GluRδ2) were detected in the serum, but not in the cerebrospinal fluid in his early clinical course. It was suggested that autoantibodies against GluRδ2 might not have injured the tissue due to the immunological action, but might be induced as a consequence of cerebellar damage. Early steroid treatment for acute cerebellitis might have been effective to prevent the progress of the disease and improve the prognosis.

Keywords: Cerebellitis; Anti-glutamate receptor antibody; Steroid; Obstructive hydrocephalus

1. Introduction

Acute cerebellitis is a neurological condition consisting of nausea, headache, and loss of consciousness in addition to the acute onset of cerebellar symptoms, and sometimes accompanies fever and meningeal signs which are rarely seen in acute cerebellar ataxia (ACA) [1]. Neuroimaging studies by MRI are also useful to differentiate acute cerebellitis from ACA and other diseases.

Although the etiology of acute cerebellitis is theoretically divided into three categories, direct infection, parainfection, and postvaccination, it is difficult to distinguish these three categories clinically. Autoantibodies against the cerebellum have been detected in disorders such as non-familial olivopontocerebellar degeneration or paraneoplastic cerebellar ataxia. Glutamate receptor δ 2 (GluRδ2) is predominantly expressed in cerebellar Purkinje cells, and plays a critical role in cerebellar functions. We report a patient with acute cerebellitis who had the IgG type of anti-GluRδ2 antibodies in the serum in his early clinical course and was successfully treated with high dose corticosteroid administration.

2. Case study

A 13-year-old boy was admitted to the hospital because of severe and intermittent headache. He had a fever and mild headache six days before admission and was treated with acetaminophen. He became afebrile at the next day but complained of worsening headache.

* Corresponding author. Tel.: +81 23 628 5329; fax: +81 23 628 5332.
E-mail address: tkaze@hotmail.com (T. Shimokaze).

0387-7604/$ - see front matter © 2006 Elsevier B.V. All rights reserved.
doi:10.1016/j.braindev.2006.08.011

Two days before admission, brain computed tomography (CT) did not show any abnormalities. On neurological examination, he was alert and oriented. No cerebellar signs were observed. His routine laboratory examinations were normal. The serum β-D-glucan was not increased. Three times of rapid antigen test for influenza virus A and B were negative. A brain CT revealed low density areas in the slightly swollen left cerebellar hemisphere. A cerebrospinal fluid (CSF) study showed 404 cells/mm^3 with 94% lymphocytes; protein was 144 mg/dl; and glucose 50 mg/dl. Bacterial culture, viral culture, and cryptococcal antigen were negative. CSF polymerase chain reaction (PCR) analysis did not detect Herpes simplex virus DNA. He progressively developed nausea, vomiting, photophobia, nuchal rigidity, and severe headache. Brain magnetic resonance imaging (MRI) revealed cerebellitis of the left hemisphere and obstructive hydrocephalus (Fig. 1). The serum antibody and PCR analysis for *Coxiella burnetii* did not indicate Q fever. A CSF study did not show an increase in the concentration of myelin basic protein or an oligoclonal band; however, the anti-GluRδ2 antibodies were detected in the serum (Table 1). He was treated with 1 g/day of intravenous methylprednisolone for three days. His meningeal signs soon disappeared; however, he transiently showed mild dysmetria and dysdiadochokinesis on the left side. He left hospital on the 21st day of his illness without any sequelae. After six months, his neurological signs were normal and the serum anti-GluRδ2 antibodies were negative, but his brain MRI showed mild atrophy of the left cerebellar hemisphere (Table 1, Fig. 2).

Fig. 1. Axial T2-weighted image on the 11th day of illness shows increased signal intensity in the left cerebellar hemisphere and compression of the fourth ventricle.

Table 1
Autoantibodies against glutamate receptor ε and δ2

Sample	The day after onset	IgG-ε2	IgM-ε2	IgG-δ2	IgM-δ2
CSF	Day 11	–	–	–	–
Serum	Day 10	–	–	+	–
Serum	6 month	–	–	–	–

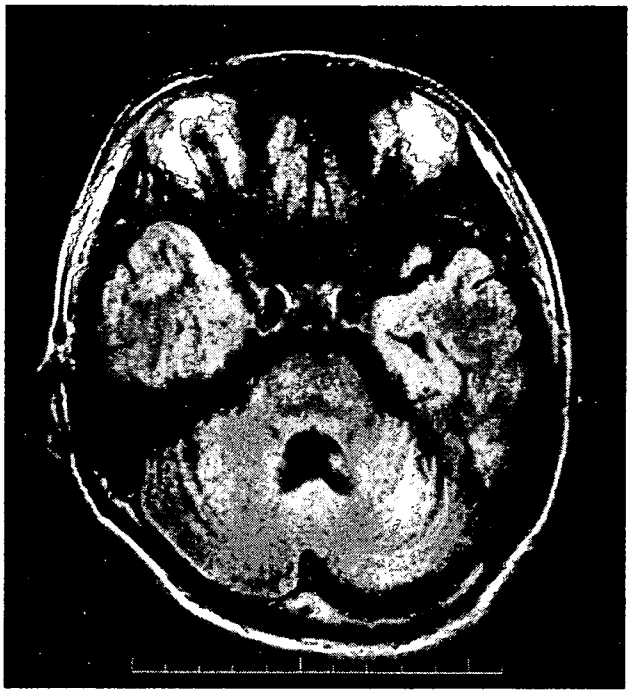

Fig. 2. Axial fluid attenuated inversion recovery image after six months shows increased signal intensity and mild atrophy in the left cerebellar hemisphere.

3. Discussion

The patient had fever and headache as initial symptoms and developed cerebellar signs after steroid therapy. Patients with acute cerebellitis initially show headache, vomiting, and disturbances of consciousness, similar to our patient [1]. Fever and stiff neck might be also seen in acute cerebellitis, but cerebellar signs are sometimes hidden by those symptoms in the first stage of illness [1]. Pleocytosis in the CSF and stiff neck indicated meningitis in our patient, and dilatation of the ventricles and high signal intensity areas around the lateral ventricles on the T2 weighted MRI image suggested increased intracranial pressure caused by cerebellar swelling and obstruction of the aqueduct. Both pathological conditions induced headache and disturbance of consciousness, which were critical points to segregate acute cerebellitis from ACA.

Neither viral nor bacterial agents have been isolated in our patient, as reported in 70% patients with acute cerebellitis. EB virus and Varicella-zoster virus are responsible for acute cerebellitis [1]. Interestingly, anti-ganglioside antibodies (GM1, GM2, and GT1b) have been detected in the serum from a patient with meningo-encephalitis and cerebellitis due to *Mycoplasma pneumoniae* infection [2]. Gangliosides are the sphingoglycolipids with sialic acid, which are located predominantly in nuclear areas of gray matter, and a small amount in the myelin of white matter [3]. Although the mechanism by which antibodies to glycolipids are induced by Mycoplasma pneumoniae infection is not clear, common epitopes might exist in neurons and Mycoplasma pneumoniae [2]. In our case, serologic test for Mycoplasma pneumoniae was not performed because of lacking overt pneumonia signs. Recently, molecular mimicry has been shown between the bacterial lipo-oligosaccharide, the cell-surface structure of *Campylobacter jejuni*, which is the most frequent antecedent pathogen for axonal type of Guillain-Barré syndrome, and the human gangliosides, GM1 or GD1a, expressed in the peripheral nerves [4]. Efforts to detect a specific pathogen and comparative analysis of the molecular structure between the pathogen and cerebellar neurons seem to be important to understand the pathogenesis of acute cerebellitis.

Besides anti-ganglioside antibodies, several types of autoantibodies have been detected in neurological conditions involved in the cerebellum, e.g., anti-Yo or anti-Hu antibodies in paraneoplastic cerebellar ataxia and anti-ZIC1 antibody in cerebellar degeneration [5,6]. Autoantibodies against glutamate receptors have been reported in the chronic form of epilepsy syndrome, such as Rasmussen encephalitis or epilepsia partialis continua [7]. The IgG type of anti-GluRδ2 antibodies were identified in the sera, but not in the CSF in our patient. So far, anti-GluRδ2 antibody has been found in patients with a chronic course of cerebellitis [8] and acute encephalitis [9]. In a patient with chronic cerebellitis, both IgG and IgM of GluRδ2 antibodies were detected in the CSF from the initial stage [8], which was different from our patient. Autoimmunity against GluRδ2 was not likely a cause for acute cerebellitis in our patient because of the absence of anti-GluRδ2 antibodies in the CSF. Although the precise mechanism by which anti-GluRδ2 antibodies were induced is unclear, infection by an unknown agent might have caused meningitis and cerebellitis, which led to a massive leakage of cerebellar antigens, including GluRδ2, and consequently induced autoantibodies against GluRδ2. The patient with chronic cerebellitis received intravenous immunoglobulin treatment at one month after the onset of the disease [8]. Early treatment may prevent the development of the injury by the immunological reaction. It was reported that high dose steroid therapies might improve the symptoms and avoid neurosurgical decompression [10]. Early steroid treatment for acute cerebellitis is likely effective to prevent the progress of cerebellitis and to improve the prognosis. Further investigation would be required to understand the role of autoantibodies in the pathogenesis of acute cerebellitis.

References

[1] Sawaishi Y, Takada G. Acute cerebellitis. Cerebellum 2002;1:223–8.
[2] Komatsu H, Kuroki S, Shimizu Y, Takada H, Takeuchi Y. *Mycoplasma pneumoniae* meningoencephalitis and cerebellitis with antiganglioside antibodies. Pediatr Neurol 1998;18:160–4.
[3] Svennerholm L. The Gangliosides. J Lipid Res 1964;5:145–55.
[4] Yuki N. Carbohydrate mimicry: a new paradigm of autoimmune diseases. Curr Opin Immunol 2005;17:577–82.
[5] Voltz R. Paraneoplastic neurological syndromes: an update on diagnosis, pathogenesis, and therapy. Lancet Neurol 2002;1:294–305.
[6] Bataller L, Wade DF, Fuller GN, Rosenfeld MR, Dalmau J. Cerebellar degeneration and autoimmunity to zinc-finger proteins of the cerebellum. Neurology 2002;59:1985–7.
[7] Takahashi Y, Mori H, Mishina M, Watanabe M, Kondo N, Shimomura J, et al. Autoantibodies and cell-mediated autoimmunity to NMDA-type GluRepsilon2 in patients with Rasmussen's encephalitis and chronic progressive epilepsia partialis continua. Epilepsia 2005;46(Suppl. 5):152–8.
[8] Sugiyama N, Hamano S, Mochizuki M, Tanaka M, Takahashi Y. A case of chronic cerebellitis with anti-glutamate receptor delta 2 antibody (in Japanese). No To Hattatsu 2004;36:60–3.
[9] Mochizuki Y, Mizutani T, Isozaki E, Ohtake T, Takahashi Y. Acute limbic encephalitis: a new entity? Neurosci Lett 2006;394:5–8.
[10] Gohlich-Ratmann G, Wallot M, Baethmann M, Schaper J, Roggendorf M, Roll C, et al. Acute cerebellitis with near-fatal cerebellar swelling and benign outcome under conservative treatment with high dose steroids. Eur J Paediatr Neurol 1998;2:157–62.

Clin Rheumatol (2007) 26:1917–1919
DOI 10.1007/s10067-007-0698-7

BRIEF REPORT

Chronic myositis with cardiomyopathy and respiratory failure associated with mild form of organ-specific autoimmune diseases

K. Tanaka · A. Sato · K. Kasuga · M. Kanazawa · K. Yanagawa · M. Umeda · M. Tada · M. Tanaka · M. Nishizawa

Received: 15 June 2007 / Revised: 25 June 2007 / Accepted: 27 June 2007 / Published online: 3 August 2007

Abstract We report the four patients with chronic myositis characterized by a very slow progression with cardiomyopathy and frequently with marked respiratory muscle weakness associated with other organ-specific autoimmune diseases such as primary biliary cirrhosis. The histopathology of the muscle showed many degenerative and regenerative fibers, but inflammatory-cell infiltration were minimal. The patients showed favorable response to high-dose corticosteroid treatment. Because of these clinical features, these patients are sometimes misdiagnosed as muscular dystrophy and not treated properly. It is important to distinguish this type of treatable myositis.

Keywords Cardiomyopathy · Chronic myositis · Primary biliary cirrhosis · Respiratory muscle weakness · Scleroderma

Introduction

The inflammatory myopathies comprise three major subsets: polymyositis (PM), dermatomyositis (DM), and sporadic inclusion-body myositis (IBM). Pure PM is a rare disorder differentiated from DM by skin involvement and muscle pathology. The underlying pathophysiologies are presumed to be different because CD8+ cytotoxic T lymphocytes (CTL) have a major role in PM, whereas humoral pathophysiologies are suspected in DM [1, 2].

PM and DM develop subacutely within several weeks to several months, typically showing proximal limb muscle weakness with dysphagia and usually the serum creatine kinase (CK) is elevated. The muscle pathology commonly seen in PM and DM are muscle fiber necrosis, degeneration, regeneration, phagocytosis, and inflammatory-cell infiltration. However, in PM, the endomysial infiltrates are mostly within the fascicles surrounding normal-appearing muscle fibers resulting in phagocytosis and necrosis without perifascicular atrophy, whereas in DM, the endomysial inflammation is predominantly perivascular and the presence of perifascicular atrophy is the characteristic feature of DM. PM or DM sometimes develop together with other autoimmune disorders, such as Sjögren syndrome, systemic scleroderma, or rheumatoid arthritis as an overlapping syndrome.

On the other hand, there are several types of chronic myositis, among IBM occurs most frequently [3]. We present in this study four patients with chronic myositis with certain characteristics other than IBM associated with mild to subclinical autoimmune disorders, such as primary biliary cirrhosis (PBC).

K. Tanaka (✉) · A. Sato · K. Kasuga · M. Kanazawa · K. Yanagawa · M. Umeda · M. Tada · M. Nishizawa
Department of Neurology, Brain Research Institute, Niigata University, Niigata City, Niigata 951-8585, Japan
e-mail: keiko@bri.niigata-u.ac.jp

M. Tanaka
Department of Neurology, National Utano Hospital, Kyoto, Japan

Case presentations

Case 1 A 37-year-old woman had leg stiffness and fatigue since 1997 and had a feeling of difficulty in climbing stairs in January 2001. In May 2002, she had a baby by normal delivery, at which time she was diagnosed as having arrhythmia. After the delivery, she had difficulty in getting up from bed and had muscle pain in the thigh and upper

arms. She lost 10 kg in the last 4 months, and her generalized muscle atrophy exacerbated. Her respiration was very weak without visible thoracic movement. On admission in October 2002, she was somnolent and had difficulty in swallowing and mild weakness of neck flexion and proximal limb muscles. She had a waddling gait and was unable to stand up from a sitting position. Her serum CK level was 4,207 IU/l. She had mild polycythemia because of chronic hypoxemia. Her vital capacity was low. She also showed mildly elevated serum IgM level (277 mg/dl). She was weakly positive for the anti-mitochondrial antibody (AMA), positive for anti-thyroid peroxidase (TPO)-antibody and anti-thyroglobulin (Tg) antibody. Her thyroid hormone levels were normal. She was negative for anti-Scl-70, anti-Jo-1, anti-centromere antibodies. Chest computed tomography (CT) showed no interstitial pneumonitis (IP). Electrocardiogram (ECG) showed atrial and ventricular premature contractions (VPC) and an echocardiogram showed left ventricular hypomotility. She was treated with high-dose prednisolone, and the serum CK level gradually decreased; however, muscle weakness or respiratory disturbance did not improve. She was then treated with four courses of methylprednisolone pulse therapy (mPulse, 1 g/day for 3 days) with Bi-level positive airway pressure (BiPAP) and high-dose oral prednisolone during her hospitalization for 9 months during which period her respiratory function gradually returned close to normal without BiPAP, and her limb power also gradually returned close to normal with a normal serum CK level.

Case 2 A 60-year-old woman had a feeling of fatigue of the thigh muscles for the past 16 years. During this period, a high serum CK level had been noted several times, but she was not examined further. Three years before admission, she was diagnosed as having PBC by liver biopsy examination without an elevation of AMA level. On admission, she had a severe heart failure with multifocal VPC, atrioventricular block, and dilated cardiomyopathy with an ejection fraction of 44.2%. Her muscle power was mildly weak in proximal muscles [manual muscle test (MMT) scores, 4–5], and the neck flexion was severely disturbed (MMT score, 2). The serum CK level was 1,631 IU/l. Shortly after admission, she died of septic shock. An autopsy revealed myositis of the skeletal muscles and also the heart muscles.

Case 3 A 77-year-old woman was easily fatigued for the past several years. She was admitted to our hospital for general examination when she became unable to get out from bed by herself. Her MMT score were 4–5 with severe generalized muscle atrophy. The serum CK level was 1,875 IU/l. Blood gas analysis revealed hypoxemia and hypercapnea. ECG showed atrial fibrillation and multiple VPC. Chest CT showed cardiomegaly but no IP. She had the anti-centromere antibody without AMA, anti-Jo-1, or other autoantibodies. She was treated with two courses of mPulse therapy with BiPAP and high-dose oral prednisolone. She gradually improved during the follow-up period of 6 months.

Case 4 A 52-year-old woman had Raynaud's phenomenon since the age of 38. She also complained of myalgia and fatigue in all her extremities since then. She was noted to have a high serum CK level several times during that period. At 48, she was diagnosed as having calcinosis, Raynaud's phenomenon, esophageal dysmotility, sclerodactyly and telangiectasia (CREST) syndrome, and Hashimoto's thyroiditis on the basis of laboratory findings. Her serum CK level was persistently high (more than 2,000 IU/ml) and general muscle atrophy progressed. On admission, she was very thin but with mild muscle weakness. Her serum CK and anti-centromere antibody levels were high, but AMA was absent. Blood gas analysis revealed mild hypercapnea. ECG revealed atrial fibrillation and multiple VPC. Chest CT showed no IP. Prednisolone treatment was immediately started, resulting in a gradual decrease in serum CK level to the normal level and complained no fatigue.

Table 1 Clinical features of our present four patients

	Patient			
Age/sex	37/woman	60/woman	77/woman	52/woman
Initial symptoms	Fatigue	Fatigue	Fatigue	Leg pain
Years before diagnosis	5	16	Several	14
Muscle involvement	Neck Proximal limb	Neck Proximal limb	Neck Proximal limb	Neck Proximal limb
CK (IU/l)	4207	1631	1875	1071
$PaO_2/PaCO_2$ (mmHg)	54.9/76.7		44.5/74.0	82.2/44.9
Cardiac involvement	APC, VPC cardiomyopathy	AV block,VPC cardiomyopathy	Af, VPC, Cardiomegaly	Af, VPC
AMA/other autoantibody	+/+	−/− biopsy-proven PBC	−/+	−/+
Response to PSL Tx	Good	n.d. (death of septic shock)	Fair	Good

APC Atrial premature contraction, *VPC* ventricular premature contraction, *AV block* atrioventricular block, *Af* atrial fibrillation, *AMA* anti-mitochondrial antibody, *PBC* primary biliary cirrhosis, *PSL* prednisolone, *n.d.* not done

Histopathology of biopsied muscle

The histopathological findings of biopsied muscles of each patient were similar, namely, scattered degenerative and regenerative fibers at various stages and numerous central nuclei with mild inflammatory infiltration. The CD4+ T cells/CD8+ T cells/macrophages are equally infiltrated, which differed from CD8+ T cell dominant PM. Some of the muscle fibers were positive for HLA class I immunostaining.

Discussion

We report in this paper the cases of four patients with chronic myositis characterized by (1) very slow progression (from several years to nearly 20 years), (2) generalized muscle atrophy with mild limb weakness, (3) marked respiratory muscle weakness, (4) moderate to severe cardiomyopathy, (5) muscle histopathological findings indicative of chronic myositis with minimal inflammatory infiltration, sometimes with a focal accumulation of lymphocytes in the perimysium, and (6) an associated subclinical/mild form of organ-specific autoimmune diseases, such as PBC, chronic thyroiditis, and focal sclerodermia. They responded to long-term high-dose glucocorticoid administration (Table 1).

Myositis with similar features have been reported in the literature (24 cases); most of them are associated with PBC [4–6]. These 24 cases comprised of 3 men and 21 women, aged 27 to 68 years, and the periods before diagnosis took 3 to 13 years. All of them showed neck and proxymal muscle weakness including paraspinal muscles, and seven out of ten patients were described as showing severe respiratory and cardiac dysfunction. There serum CK was 258–3,565 IU/l, and all but one patient were AMA positive who all responded to prednisolone treatment, as similar to those of our present patients. Some of the reported cases were diagnosed as PBC by liver biopsy, suggesting that this group of myositis is closely related to PBC. A patient who was negative for AMA underwent liver biopsy, and the histopathological findings were compatible with PBC.

Two of our present patients were AMA-negative and anti-centromere antibody positive with normal liver functions, thus could not be diagnosed as PBC-associated myositis, although these two patients did not undergo liver biopsy.

PBC is frequently associated with other autoimmune diseases, but myositis is very rarely associated. However, these myositis patients found in the literature had features similar to those of our present four patients.

Anti-centromere antibody is frequently found in the CREST syndrome, which is sometimes associated with PBC [7]. Although it does not necessarily associated with PBC or CREST syndrome, myositis associated with these mild form of organ-specific autoimmune diseases were suggested to have similar pathophysiological mechanisms of a mild, chronic course of the autoimmune process.

In general, chronic myositis can be classified into several groups, among them IBM occurs most frequently. Pure PM not treated properly at the beginning shows an indolent course. PM itself in an overlapping syndrome with systemic lupus erythematosus or rheumatoid arthritis could not be distinguished from pure PM occurring subacutely. The myositis we presented in this paper developed subclinically over long periods together with other underlying autoimmune diseases and reached a disabling state, at which point it is difficult to distinguish it from adult-onset muscular dystrophy although with the histological examination of muscles. It is important to identify this type of chronic myositis at an early stage, as it responds well to high-dose glucocorticoid treatment.

References

1. Arahata K, Engel AG (1988) Monoclonal antibody analysis of mononuclear cells in myopathies: IV. Cell-mediated cytotoxicity and muscle fiber necrosis. Ann Neurol 23:168–173
2. Dalakas MC (2004) Inflammatory disorders of muscle: progress in polymyositis, dermatomyositis and inclusion body myositis. Curr Opin Neurol 17:561–567
3. Griggs RC, Askanas V, DiMauro S, Engel A, Karpati G, Mendell JR, Rowland LP (1995) Inclusion body myositis and myopathies. Ann Neurol 38:705–713
4. Matsui K, Aizawa Y, Inoue K, Yaguchi H, Toda G (2000) Polymyositis with marked paravertebral muscle atrophy in patients with primary biliary cirrhosis. Clin Neurol 40:694–700
5. Migueletto BC, Neto AE, Domingues EZ, Neves de Castro PP, Stocker H, Marie SK, Meireles LP, Arai MH (1999) Primary biliary cirrhosis and myopathy: An uncommon association. Rev Hosp Clin Fac Med Sao Paulo 54:165–168
6. Varga J, Heiman-Patterson T, Munoz S, Love LA (1993) Myopathy with mitochondrial alterations in patients with primary biliary cirrhosis and antimitochondrial antibodies. Arthritis Rheum 36: 1468–1475
7. Abraham S, Begum S, Isenberg D (2004) Hepatic manifestations of autoimmune rheumatic diseases. Ann Rheum Dis 63:123–129

Anti-aquaporin 4 antibody in selected Japanese multiple sclerosis patients with long spinal cord lesions

K Tanaka[1], T Tani[1], M Tanaka[2], T Saida[2], J Idezuka[3], M Yamazaki[4], M Tsujita[4], T Nakada[5], K Sakimura[4] and M Nishizawa[1]

Multiple sclerosis (MS) in Asian populations is often characterized by the selective involvement of the optic nerve (ON) and spinal cord (SP) (OSMS) in contrast to classic MS (CMS), where frequent lesions are observed in the cerebrum, cerebellum or brainstem. In Western countries, inflammatory demyelinating disease preferentially involving the ON and SP is called neuromyelitis optica (NMO). Recently, Lennon *et al.* discovered that NMO-IgG, shown to bind to aquaporin 4 (AQP4), could be a specific marker of NMO and also of Japanese OSMS whose clinical features were identical to NMO having long spinal cord lesions extending over three vertebral segments (LCL). To examine this antibody in larger populations of Japanese OSMS patients in order to know its epidemiological and clinical spectra, we established an immunohistochemical detection system for the anti-AQP4 antibody (AQP4-Ab) using the AQP4-transfected human embryonic kidney cell line (HEK-293) and confirmed AQP4-Ab positivity together with the immunohistochemical staining pattern of NMO-IgG in approximately 60% of Japanese OSMS patients with LCL. Patients with OSMS without LCL and those with CMS were negative for this antibody. Our results accorded with those of Lennon *et al.* suggest that Japanese OSMS with LCL may have an underlying pathogenesis in common with NMO. *Multiple Sclerosis* 2007; **13**: 850–855. http://msj.sagepub.com

Key words: aquaporin 4 water channel; long spinal cord lesion; neuromyelitis optica; NMO-IgG; opticospinal multiple sclerosis

Introduction

Multiple sclerosis (MS) is an inflammatory demyelinating disease of the central nervous system (CNS) probably caused by autoimmune mechanisms. MS in Asian populations is often characterized by the selective involvement of the optic nerve and spinal cord with few or no lesions observed in the cerebrum or cerebellum. This optic-spinal MS (OSMS) is in marked contrast to classic MS (CMS), where lesions are frequently observed in the cerebrum, cerebellum or brainstem, as well as in the optic nerve and spinal cord, though the definition of OSMS tends to be wider, to include small cerebral/brainstem lesions [1].

In Western countries, the inflammatory disease of the CNS that preferentially affects the optic nerve and spinal cord while virtually sparing the brain is called neuromyelitis optica (NMO), also called Devic's syndrome [2–4].

Clinicopathological features that constitute the core of OSMS [5] and NMO [4] are very similar and the question has been raised whether these two conditions are the same.

Recently, Lennon *et al.* have reported that the serum immunoglobulin G antibody (NMO-IgG) that recognizes the aquaporin-4 water channel is a specific marker of NMO [6,7]. To define the frequency and clinical characteristics of Japanese MS with this

[1] Department of Neurology, Brain Research Institute, Niigata University, Niigata Japan
[2] Department of Neurology, Utano National Hospital, Kyoto, Japan
[3] Department of Neurology, Ojiya Sakura Hospital, Ojiya, Japan
[4] Department of Cellular and Neurobiology, Brain Research Institute, Niigata University, Niigata, Japan
[5] Center for Integrated Human Brain Science, Brain Research Institute, Niigata University, Niigata, Japan
Author for correspondence: Keiko Tanaka, Department of Neurology, Brain Research Institute, Niigata University, 1-757 Asahimachi-Dori, Niigata City, Niigata 951-8585, Japan. E-mail: keiko@bri.niigata-u.ac.jp
Received 29 August 2006; accepted 16 January 2007

 10.1177/1352458507076976

antibody, we established a detection system for the anti-aquaporin-4 antibody (AQP4-Ab) immunohistochemically using AQP4-transfected culture cells together with the immunohistochemical staining of rodent and human brains and spinal cord sections (NMO-IgG detection).

Since NMO-IgG-positive patients shown in the study by Lennon *et al.* most frequently had MRI spinal-cord lesion extending over three vertebral segments (LCL), we selected MS patients with LCL for the AQP4-Ab test to validate our detection system comparing them with those without LCL or other inflammatory neurological diseases. We found that approximately 60% of MS patients with LCL have both the AQP4-Ab and immunohistochemically proven NMO-IgG, whereas no MS patients without LCL or other controls have this antibody. Our results were similar to the frequency of NMO-IgG found in NMO patients and also in Japanese OSMS patients reported by Nakashima *et al.* [8], and confirmed the results of Lennon *et al.* [6,7]. Our AQP4-Ab detection system could be a useful tool for the clinical study of MS.

Subjects and methods

Patients

To validate our AQP4-Ab detection system and compare the results with NMO-IgG study, we examined sera from 26 OSMS patients with LCL (one man and 25 women; mean age, 43.5 ± 12.3 years) mainly presenting with optic nerve and spinal cord lesions, six OSMS patients without LCL (three men and three women; mean age, 41.2 ± 10.5 years). For controls, the sera from 21 CMS patients mainly presenting with cerebral lesions (four men and 17 women; mean age, 39.9 ± 14.2 years), 28 patients with other inflammatory neuromuscular diseases such as systemic lupus erythematosus (SLE), Sjögren's syndrome (Sjs), mixed connective tissue disease (MCTD), Lambert Eaton myasthenic syndrome (LEMS), dermatomyositis, sarcoidosis and polyarteritis nodosa (seven men and 21 women; mean age, 36.1 ± 14.0 years) and 10 healthy volunteers (two men and eight women; mean age, 37.7 ± 10.3 years) were examined. Sera and CSF were obtained after receiving spoken consent for testing, and the antibody testing was performed blinded.

AQP4-Ab production

We raised a polyclonal antibody against human AQP4 in rabbits immunized with a synthetic peptide (C-terminal of human AQP4 at amino acids 301–318) and affinity-purified it. The procedures used for immunization and antibody purification were reported previously [9]. This AQP4-Ab cross-reacted with mouse AQP4; therefore, its specificity was confirmed using an AQP4 knockout mouse. To examine staining patterns, paraffin-embedded sections or cryostat sections of the human cerebrum, cerebellum and spinal cord were stained with the raised antibody.

Cloning of human AQP4 and expression in cultured cells

Total RNA was extracted from an adult human cerebellum using ISOGEN (Nippongene). cDNA encoding human aquaporin 4 (AQP4 M23 isoform; GenBank accession number U63623 [10]) was cloned by the reverse-transcription polymerase chain reaction (RT-PCR) technique. First-strand cDNA was synthesized from human brain total RNA using an Advantage RT-for-PCR kit (Clontech). Full-length cDNA was inserted into the *Xba*I site of a pEF-BOS expression vector. HEK 293 cells were seeded in Dulbecco's modified Eagle's medium (DMEM) containing 10% fetal calf serum (FCS) one day before transfection at 3×10^4 cells per well in a poly-L-lysine-coated eight-well chamber slide (BD BioCoat). The cells were transfected with an AQP4 expression vector or a control empty vector using lipofectamine reagent (Invitrogen) according to the manufacturer's instructions.

Immunohistochemistry

Thirty hours after transfection, the HEK-293 cells were fixed in 4% paraformaldehyde in 0.1 M phosphate-buffered saline (PBS, pH 7.4) for 20 minutes. Then, non-specific binding was blocked with 10% goat serum/PBS, and the cells were incubated with a patient's serum (1:20–1:1000), cerebrospinal fluid (CSF, 1:1–1:10) or the rabbit antibody for the human AQP4-peptide (0.3 μg/mL) for 60 minutes at room temperature, then incubated with fluorescein isothiocyanate (FITC)-conjugated rabbit anti-human IgG (BD Biosciences) for a patient's serum or CSF and FITC-conjugated goat anti-rabbit IgG for a rabbit serum, for 30 minutes. Then, a *SlowFade* Gold antifade reagent (Molecular Probes, USA) was applied to the slide. Between steps, the wells were washed with PBS three times.

To confirm the coincidence of staining pattern between MS sera and AQP4-Ab raised in rabbits, rhodamine-conjugated goat anti-rabbit IgG (BD Biosciences) was used as the secondary antibody for the latter.

Cryostat sections (8 μm thick) of the rat cerebrum, cerebellum or human spinal cord were immunostained as follows: tissue sections were air-dried, fixed in cold acetone for 10 minutes, and blocked with 10% goat serum/PBS, MS or control serum (1:20–1:1000) for 60 minutes, then with FITC-anti-human IgG (BD Biosciences), followed by a *SlowFade* Gold antifade reagent was applied. Between steps, the sections were washed with PBS three times.

Results

The AQP4-Ab raised against the AQP4 peptide in the rabbit reacted with the microvessel wall, pia, subpia and margin of the Virchow-Robin space in the human cerebrum and cerebellum, producing a staining pattern the same as that of NMO-IgG [6]; thus, we used this antibody as the positive control.

The AQP4-Ab in the sera of MS patients reacted with the AQP4-transfected HEK-293 cells, showing a dotlike staining pattern on the cell surface and along cell processes, but not with the non-AQP4-transfected HEK cells (*Figure 1*). The efficiency of AQP4 transfection in the HEK-293 cells was very stable between transfections, at 35.8 ± 1.2%, determined with the same serum used as the positive control for each staining examination.

Rat or human cerebrum, cerebellum and spinal cord cryostat sections were incubated with the AQP4-Ab-positive MS serum examined by AQP4-transfected HEK-293 cell immunostaining and gave similar staining patterns to NMO-IgG (Figure 2).

AQP4-Ab positivity was observed in 16 of 26 patients diagnosed as OSMS with LCL but in none of the six OSMS patients without LCL. The patients with CMS and other inflammatory neuromuscular diseases and the healthy controls were all negative for AQP4-Ab. No sera reacted with the non-AQP4-transfected HEK-293 cells.

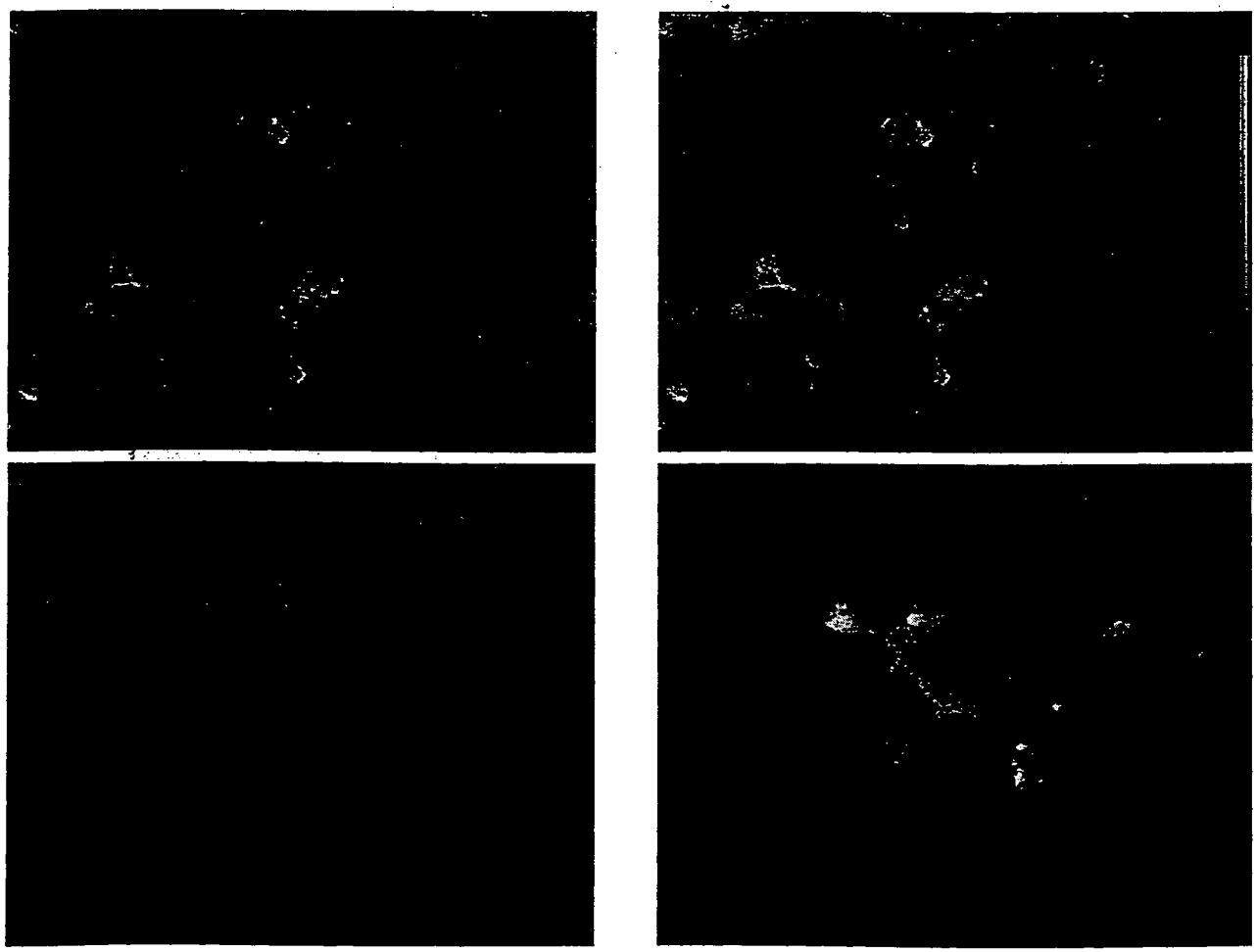

Figure 1 Immunostaining of AQP4-transfected HEK-293 cells with AQP4-Ab. LCL(+)MS serum (1 : 400)/FITC-anti-human IgG (top left), affinity-purified rabbit IgG specific for human AQP4 C-terminal peptide (0.3 μg/mL)/Rhodamine-anti-rabbit IgG (top right), merged figure (bottom left) and high power figure of LCL(+)MS serum/FITC-anti-human IgG.

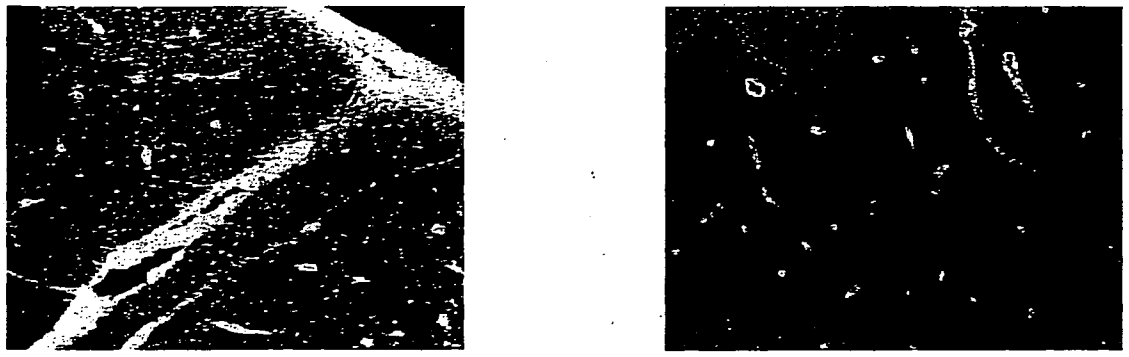

Figure 2 Immunostaining of rat cerebrum with LCL(+)MS serum (1 : 1000). The pia, subpia and perivascular area (high power) were identical to NMO-IgG staining.

All 16 AQP4-Ab-positive patients had LCL extending over three or more vertebral longitudinal segments (LCL(+)MS), whereas 10 LCL(+)MS patients were AQP4-Ab-negative, that is 61.5% of LCL(+)MS patients were AQP4-Ab-positive (Table 1).

Comparison of AQP4-Ab-positive and AQP4-Ab-negative LCL(+)MS patients showed that the former group comprised only women with severe visual disturbance (seven were blind), whereas the latter group comprised one man and nine women, of which only one was blind. The duration of the disease was also longer in the former group at the point of this study (AQP4-Ab-positive: 12.1 ± 9.2 years; AQP4-Ab-negative: 5.9 ± 2.5 years). However the examined sera from six of the patients of this group were obtained at the early stage of the disease (less than two years from onset) so the antibody production is not secondary to a long disease course. Other factors such as mean age (AQP4-Ab-positive: 49.1 ± 13.5 years; AQP4-Ab-negative: 42.4 ± 14.8 years), severity of limb and truncal disabilities (as shown by mean value of expanded disability status scale (EDSS) score; AQP4-Ab-positive: 8.1 ± 2.1; AQP4-Ab-negative: 7.3 ± 2.5), existence of cerebral lesions (AQP4-Ab-positive: eight of 16 patients; AQP4-Ab-negative: five of 10) did not differ between the two groups (Table 2).

Table 1 Clinical phenotype of AQP4-Ab (+) patients. Sixteen of 26 OSMS patients with LCL were positive for the AQP4-Ab, while other phenotypes were all negative for the antibody

	AQP4-Ab (+)
OSMS with LCL	16/26 (61.5%)
OSMS without LCL	0/6
CMS without LCL	0/21
OND	0/28
Healthy controls	0/10

OND: other inflammatory neurological diseases.

Table 2 Clinical features of AQP4-Ab-positive or AQP4-Ab-negative LCL(+)MS patients

Study parameter	AQP4-Ab (+)	AQP4-Ab (−)
Sex (male : female)	0 : 16	1 : 9
Age at examination	49.1 ± 13.5	42.4 ± 14.8
Years from onset of disease	12.1 ± 9.2	5.9 ± 2.5
EDSS score	8.1 ± 2.1	7.3 ± 2.5
No. of patients with cerebral lesions	8/16	5/10
No. of blind patients	7/16	1/10

Of the AQP4-Ab-positive patients, half were in the active stage of the disease and some had been treated with several cycles of 1000 mg of methylprednisolone per day for three days just before sera were taken, and the other half were in a chronic stable stage without corticosteroid or immunosuppressive treatment when sera were taken. The sera were taken several times in the active and remission stages in three of the patients and the AQP4-Ab was positive in all the sera taken in the active and chronic stages.

Discussion

It has long been considered that relapsing-remitting MS in Japan could be classified into two groups: CMS and OSMS. Compared with CMS, OSMS has some distinctive features similar to those of NMO: 1) older age at onset; 2) high female-to-male ratio; 3) high relapse frequency; 4) severe disability; 5) few cerebral lesions but tend to have long spinal cord lesions; 6) pleocytosis and absence of oligoclonal bands in the cerebrospinal fluid; 7) continuous shift towards a Th1 phenotype even in the remission phase, but only in the exacerbation phase in CMS, as suggested by results obtained using several biomarkers; 8) difference in spinal

cord neuropathology, that is, swelling and cavitation observed macroscopically and large numbers of polymorphonuclear cells containing neutrophils and eosinophils with a hyalinized appearance of medium-sized arteries observed microscopically; and 9) association with systemic autoimmune disorders such as hypothyroidism, Sjögren's syndrome or other types of connective tissue disease with multiple autoantibodies [11]. With these features, Wingerchuck *et al.* concluded that NMO is distinct from MS with different underlying pathogenesis, and incorporated the new findings on NMO-IgG in their concept [12].

Following the recent reports by Lennon *et al.* [6,7], we established an AQP4-Ab detection system together with the NMO-IgG test and confirmed their results in Japanese MS: 61.5% of Japanese LCL(+)MS patients were positive for AQP4-Ab, which was similar in the frequency of NMO-IgG positivity in seven of 12 Japanese MS patients reported under the designation of OSMS (58%) [6] and also in 12 of 19 patients (63%) [8]. In the report of Nakashima *et al.*, they described two NMO-IgG-positive CMS patients [8]. They diagnosed the two patients as having CMS because they had extensive brain lesions, although they otherwise had typical features of OSMS. In our series, almost half of the LCL(+)MS patients with or without AQP4-Ab showed cerebral MRI lesions, which were unlike typical CMS, and optic or spinal cord lesions preceded several years before cerebral MRI lesions were detected. Among them, one patient showed a large cystic lesion in the cerebral white matter. The proposed diagnostic criteria for NMO exclude patients with lesions outside the optic nerve and spinal cord. However, Pittock *et al.* included patients with cerebral lesions in NMO in their recent study [13], and Wingerchuk *et al.* [11] proposed revised diagnostic criteria for NMO that will include patients with MRI brain lesions. These revised criteria brought NMO closer to LCL(+)MS.

The AQP4-Ab-positive patients tended to show severe paraplegia in the early stage of the disease; 50% of these patients became blind shortly thereafter. Only one of seven AQP4-Ab-negative patients with LCL(+)MS was blind in our series.

Whether AQP4-Ab is directly related to the pathogenesis of LCL(+)MS and NMO remains to be elucidated. It is not necessarily related directly to the presence of active demyelinating lesions because patients at the chronic stage of the disease, who showed only an atrophic spinal cord without active inflammatory lesions (no cord swelling nor gadolinium-enhanced lesions), were also AQP4-Ab-positive. This indicates that the antibody does not simply block or disturb the function of water channels, or cause edema in nervous tissues only at the acute stage. However, the presence of the antibody might disrupt the formation of severe inflammatory lesions in nervous tissues once initial pathomechanisms develop.

We used both the immunohistochemical staining pattern of CNS tissues (NMO-IgG) and a confirmatory test on specific binding to AQP4-Ab, since the NMO-IgG staining pattern itself is not equal to AQP4 antigen detection, because other proteins colocalized with AQP4 could show similar immunohistochemical staining patterns. Thus our antibody test using full-length human AQP4 cDNA-transfected HEK 293 cells is more specific for defining AQP4-Ab positivity than the immunohistochemical detection system of NMO-IgG.

AQP4 is a water-selective transporter expressed strongly in astrocytes and ependymal cells throughout the brain and spinal cord, particularly at sites of fluid transport at the pial and ependymal surfaces in contact with the cerebrospinal fluid [14,15]. AQP4 has also been shown to be expressed at the optic chiasm [16]. AQP4 is thought to be involved in the development of brain edema. There is accumulating evidences that it is related to glial migration and neural signal transduction, as obtained through many experimental studies [17,18]. In the immunohistochemical study of the MS brain using the AQP4-Ab raised against a synthetic peptide homologous to the C-terminal end of the cytoplasmic domain of the rat AQP4, the staining intensity was prominent at the periphery of the plaques of recent foci; however, this perilesional accentuation of AQP4 expression is evident even at later stages with glial scarring without edema [19]. We could not find a similar study of LCL(+)MS brains and the role of the AQP4-Ab on lesion formation in this group is not yet known. The preferential involvement of the optic nerve and spinal cord in LCL(+)MS is not yet understood. AQP4 has been shown to be expressed at a high level in the gray matter in the spinal cord where numerous AQP4-dense processes are found in direct contact with neuronal cell bodies and synapses [20,21]. There is as yet no direct comparison of AQP4 densities and their distribution in the cerebrum and the spinal cord. The interpretation of the significance of AQP4-Ab in LCL(+)MS needs to wait until more basic knowledge of AQP4 is obtained.

Acknowledgements

This study was supported in part by the Ministry of Education, Culture, Sports, Science, and Technology, Japan and a Neuroimmunological Disease Research Committee grant from the Ministry of Health, Labor, and Welfare, Japan.

References

1. **Saida T, Tashiro K, Itoyama Y, Sato T, Ohashi Y, Shao Z** *et al.* Interferon beta-1b is effective in Japanese RRMS patients: A randomized, multicenter study. *Neurology* 2005; **64**: 621–30.
2. **Cree BA, Goodin DS, Hauser SL.** Neuromyelitis optica. *Semin Neurol* 2002; **22**: 105–22.
3. **O'Riordan JI, Gallagher HL, Thompson AJ, Howard RS, Kingsley DP, Thompson EJ** *et al.* Clinical, CSF, and MRI findings in Devic's neuromyelitis optica. *J Neurol Neurosurg Psychiatry* 1996; **60**: 382–87.
4. **Wingerchuk DM, Hogancamp WF, O'Brien PC, Weinshenker BG.** The clinical course of neuromyelitis optica (Devic's syndrome). *Neurology* 1999; **53**: 1107–14.
5. **Kira J.** Multiple sclerosis in the Japanese population. *Lancet Neurol* 2003; **2**: 117–27.
6. **Lennon VA, Wingerchuk DM, Kryzer TJ, Pittock SJ, Lucchinetti CF, Fujihara K** *et al.* A serum autoantibody marker of neuromyelitis optica: distinction from multiple sclerosis. *Lancet* 2004; **364**: 2106–12.
7. **Lennon VA, Kryzer TJ, Pittock SJ, Verkman AS, Hinson SR.** IgG marker of optic-spinal multiple sclerosis binds to the aquaporin-4 water channel. *J Exp Med* 2005; **202**: 473–77.
8. **Nakashima I, Fujihara K, Miyazawa I, Misu T, Narikawa K, Nakamura M** *et al.* Clinical and MRI features of Japanese MS patients with NMO-IgG. *J Neurol Neurosurg Psychiatry* 2006; **77**: 1073–75.
9. **Watanabe M, Fukaya M, Sakimura K, Manabe T, Mishina M, Inoue Y.** Selective scarcity of NMDA receptor channel subunits in the stratum lucidum (mossy fibre-recipient layer) of the mouse hippocampal CA3 subfield. *Eur J Neurosci* 1998; **10**: 478–87.
10. **Lu M, Lee MD, Smith BL, Jung JS, Agre P, Verdijk MAJ** *et al.* The human *AQP4* gene: definition of the locus encoding two water channel polypeptides in brain. *Proc Natl Acad Sci USA* 1996; **93**: 10908–12.
11. **Wingerchuk DM, Lennon VA, Pittock SJ, Lucchinetti CF, Weinshenker BG.** Revised diagnostic criteria for neuromyelitis optica. *Neurology* 2006; **66**:1485–89.
12. **Wingerchuk DM.** Neuromyelitis optica. In Freedman MS ed. *Advances in neurology* (Vol 98). Lippincott Williams & Wilkins, 2006: 319–33.
13. **Pittock SJ, Lennon VA, Krecke K, Wingerchuk DM, Lucchinetti CF, Weinshenker BG.** Brain abnormalities in neuromyelitis optica *Arch Neurol* 2006; **63**: 390–96.
14. **Nielsen S, Nagelhus ER, Amiry-Moghaddam M, Bourque C, Agre P, Ottersen OP.** Specialized membrane domains for water transport in glial cells: High-resolution immunogold cytochemistry of aquaporin-4 in rat brain *J Neurosci* 1997; **17**: 171–80.
15. **Rash JE, Yasumura T, Hudson CS, Agre P, Nielsen S.** Direct immunogold labeling of aquaporin-4 in square arrays of astrocyte and ependymocyte plasma membranes in rat brain and spinal cord *Proc Natl Acad Sci USA* 1998; **95**: 11981–86.
16. **Venero JL, Vizuete ML, Ilundáin AA, Machado A, Echevarria M, Cano J.** Detailed localization of aquaporin-4 messenger RNA in the CNS: preferential expression in periventricular organs *Neurosci* 1999; **94**: 239–50.
17. **Verkman AS.** More than just water channels: unexpected cellular roles of aquaporins. *J Cell Sci* 2005; **118**: 3225–32.
18. **Verkman AS, Binder DK, Bloch O, Auguste K, Papadopoulos MC.** Three distinct roles of aquaporin-4 in brain function revealed by knockout mice. *Biochim Biophys Acta* 2006; (online).
19. **Aoki-Yoshino K, Uchihara T, Duyckaerts C, Nakamura A, Hauw J-J, Wakayama Y.** Enhanced expression of aquaporin 4 in human brain with inflammatory diseases. *Acta Neuropathologica* 2005; **110**: 281–88.
20. **Oshio K, Binder DK, Yang B, Schecter S, Verkman AS, Manley GT.** Expression of aquaporin water channels in mouse spinal cord. *Neurosci* 2004; **127**: 685–93.
21. **Vitellaro-Zuccarello L, Mazzetti S, Bosisio P, Monti C, De Biasi S.** Distribution of Aquaporin 4 in rodent spinal cord: Relationship with astrocyte markers and chondroitin sulfate proteoglycans. *Glia* 2005; **51**: 148–59.

SHORT REPORT

Anti-aquaporin 4 antibody in Japanese multiple sclerosis: the presence of optic–spinal multiple sclerosis without long spinal cord lesions and anti-aquaporin 4 antibody

Masami Tanaka, Keiko Tanaka, Mika Komori, Takahiko Saida

J Neurol Neurosurg Psychiatry 2007;**78**:990–992. doi: 10.1136/jnnp.2006.114165

Background: Anti-aquaporin 4 (AQP4) antibodies were found in patients with neuromyelitis optica (NMO) and Japanese optic–spinal multiple sclerosis (OSMS).
Objective: To review the clinical features and investigate anti-AQP4 antibodies of Japanese patients with multiple sclerosis (MS), with or without long spinal cord lesions (LCL).
Methods: Anti-AQP4 antibodies were examined in the sera of 128 consecutive Japanese patients by the immunofluorescence method using AQP4 transfected cells.
Results: The 45 LCL-MS patients included 28 with a long spinal cord lesion extending contiguously over three vertebral segments on sagittal T2 weighted images (long T2 lesion) and 17 with segmental cord atrophy extending more than three vertebral segments. We identified 25 patients with anti-AQP4 antibody with LCL and anti-AQP4 antibody. Anti-AQP4 antibody was found in 12/17 (70.6%) LCL-MS patients with segmental cord atrophy, and in 13/28 (46.4%) LCL-MS patients without segmental long cord atrophy ($p=0.135$, Fisher's exact test). Seropositive MS patients with LCL had more relapses than seronegative patients ($p=0.0004$, Mann–Whitney U test). 9 patients with OSMS were negative for anti-AQP4 antibody who did not show LCL.
Conclusion: These results suggest that an anti-AQP4 antibody is found not only in MS patients with long T2 lesions but also in patients with segmental cord atrophy extending more than three vertebral segments. It is a marker of LCL-MS showing frequent exacerbations. Japanese OSMS cases comprised those that were identical to NMO cases and those that were more closely related to classic MS.

Multiple sclerosis (MS) is a chronic autoimmune disorder of the central nervous system. Japanese MS patients have been classified into two phenotypes: classic MS (CMS) and optic–spinal MS (OSMS).[1] OSMS has been recognised since the 1950s.[2] Patients with OSMS have symptoms and MRI findings in which the main lesions are confined to the optic nerve and spinal cord. In patients with OSMS, there is a higher female/male ratio; neuropathologically necrotic lesions; pleocytosis with a predominance of polymorphonuclear cells and a low frequency of oligoclonal IgG bands in CSF; a high incidence of autoantibodies in sera; long spinal cord lesions (LCL) extending more than three vertebral segments in MRI scans; and an association with a human leucocyte antigen class II allele (DPB1*0502).[3]

Neuromyelitis optica (NMO) has been described as Devic disease, but its clinical definition has frequently been revised.[4] LCL extending contiguously over three vertebral segments on sagittal T2 weighted images (long T2 lesion) is a disease marker. Current NMO criteria include unilateral optic neuritis, no restriction on onset of optic neuritis and myelitis, relapsing course and brain involvement.[4 5] Recent NMO criteria stress the presence of both brain MRI abnormalities that do not meet diagnostic criteria for MS and NMO-IgG,[4] a highly specific biomarker of NMO,[6] and its target antigen is the aquaporin 4 (AQP4) water channel.[7]

The incidence of NMO-IgG seropositivity in Japanese patients with OSMS (6/11 cases, 54%) was similar to that in NMO (33/45, 73%), and OSMS was thought to be the same disease.[6] However, in that study,[6] the Japanese OSMS patients had been selected using 1999 NMO criteria (Fujihara K, personal communication) that are not the same as the clinical definition of OSMS widely used in Japan.[8] Their recent report showed that serum NMO-IgG was found in 12 of 19 patients with OSMS (63%).[9] We established an AQP4 antibody assay system and identified nine seropositive MS patients with LCL-MS.[10]

PATIENTS AND METHODS

A total of 128 consecutive Japanese patients (36 men, 92 women), aged 21–75 years, who had definite relapsing–remitting MS clinically, according to McDonald's criteria, were considered for enrolment in our study. Patients with primary progressive MS, spinal MS and relapsing optic neuritis were excluded. Time since onset was 1–35 years. Kurtzke's Expanded Disability Status Scale (EDSS) score[11] was used for the clinical ratings.

Patients who showed selective involvement of the spinal cord and optic nerves but no clinical signs indicative of cerebrum, cerebellum or brainstem involvement were classified as having OSMS, while those with estimated lesions in the cerebrum, cerebellum or brainstem were defined as CMS.[1] Patients with a long cord lesion on spinal cord MRI (long T2 lesion or segmental cord atrophy) extending over three vertebral segments were designated as having LCL-MS.

Anti-AQP4 antibody measurement

Anti-AQP4 IgG antibody in MS patient sera was measured using an indirect immunofluorescence method reported previously[10] with HEK-293 cells transfected with an AQP4 expression vector containing full length cDNA of human AQP4. Sera were obtained during the clinically stable stage. Anti-AQP4 antibody was measured by one of the authors (KT) who was blind to all clinical information, including clinical phenotype.

The statistical significance of differences between the two groups were determined using the Mann–Whitney U test or Fisher's exact test for difference in percentage anti-AQP4 antibodies between patients with and without segmental long spinal cord atrophy.

Abbreviations: AQP4, aquaporin 4; CMS, classic multiple sclerosis; EDSS, Expanded Disability Status Scale; LCL, long spinal cord lesions; MS, multiple sclerosis; NMO, neuromyelitis optica; OSMS, optic–spinal multiple sclerosis

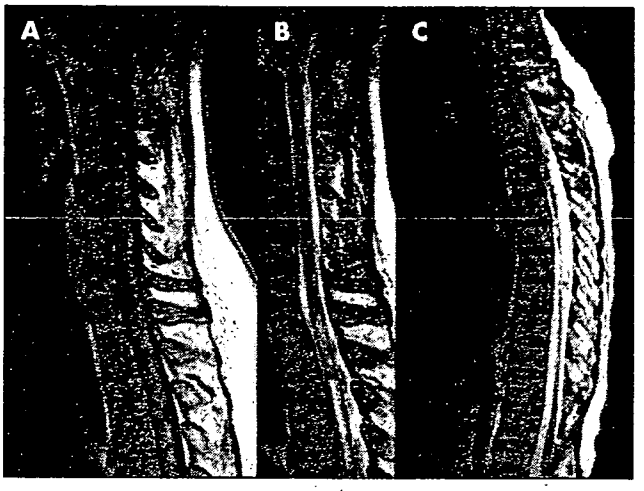

Figure 1 MRI findings of patients with long spinal cord lesions–multiple sclerosis (LCL-MS). The patient shows discontinuous enhanced lesions from C1 to Th5 (A) and discontinuous T2 high intensity lesions in the cervical segment and T2 high intensity lesions from Th1 to Th5 (long T2 lesion) (B). Another patient shows segmental spinal cord atrophy from C7 to Th11 (C).

This study was approved by the Medical Ethics Committee of Utano National Hospital. All participants gave written informed consent.

RESULTS

The 45 LCL-MS patients (five men and 40 women) included 28 with long T2 lesions (four men and 24 women) and 17 with segmental cord atrophy extending more than three vertebral segments (two men and 15 women) (fig 1). Anti-AQP4 antibodies were found in 12/17 (70.6%) LCL-MS patients with segmental cord atrophy and in 13/28 (46.4%) LCL-MS patients without segmental long cord atrophy ($p = 0.135$, Fisher's exact test) (table 1). Excluding those with LCL-MS, patients did not have anti-AQP4 antibodies. There was a relationship between blindness and seropositivity against AQP4 ($p<0.0005$) (table 2). Eleven of 128 patients were blind, nine of whom had LCL-MS. Seven of the nine blind patients had LCL and anti-AQP4 antibodies.

The number of relapses in 22 patients with LCL-MS and anti-AQP4 antibodies (0–7; mean 3.64) was greater than in 18 seronegative patients with LCL-MS (0–6; 1.39) in the year before determination of antibodies ($p = 0.0004$). Time from onset for seropositive patients (mean 14.3) was not different from that of seronegative patients (9.1) ($p = 0.1518$). There was no other difference in clinical phenotype between patients with and without anti-AQP4 antibodies.

We found nine OSMS patients who had a 5 year minimum follow-up period after onset and did not have LCL or anti-AQP4 antibodies (OSMS(−)). Age of OSMS(−) onset ranged from 7 to 51 years (mean 27.0), which did not differ from that of LCL-MS cases (2–62 years; 35.2) ($p = 0.1281$). The period after onset of OSMS (−) was 5–24 years (mean 11.4), which did not differ from that of LCL-MS cases (1–30 years; 12.0) ($p = 0.6685$). Kurtzke's EDSS for OSMS(−) (0–4.0; mean 1.50), however, was lower than that for LCL-MS (0–9.5; 6.63) ($p<0.0001$). At disease onset, one of three patients had asymptomatic subcortical white matter lesions on brain MRI, while the other two had normal brain MRI findings. However, most patients who had optic neuritis as the first event did not undergo MRI. Patients with OSMS(−) had no clinical manifestations except for symptoms or signs caused by lesion of the optic nerves or spinal cord. All showed asymptomatic brain lesions on T2 weighted brain MRI scans.

Table 1 Number of seropositive patients with multiple sclerosis

	n	No of anti-AQP4 antibody positive (%)
Total LCL-MS	45	25 (55.6%)
With segmental cord atrophy	17	12 (70.6%)
Without segmental cord atrophy	28	13 (46.4%)
OSMS	22	2 (9.1%)
Including LCL-MS	3	2 (66.7%)
CMS	64	0 (0%)
Less than 5 y after onset	29	4 (13.8%)
Including LCL-MS	9	4 (44.4%)
OSMS	9	0 (0%)

AQP4, aquaporin 4; CMS, classic multiple sclerosis—patients with estimated lesions in the cerebrum, cerebellum or brainstem; LCL-MS, long spinal cord lesions-multiple sclerosis—patients with a long spinal cord lesion on MRI (long T2 lesion or segmental cord atrophy) extending over three vertebral segments; OSMS, optic-spinal multiple sclerosis—patients with selective involvement of the spinal cord and optic nerves but no clinical signs indicative of cerebrum, cerebellum or brainstem involvement;
The 128 patients include 45 patients with LCL-MS, 12 with OSMS and 71 with CMS.

DISCUSSION

Anti-AQP4 antibody is a good diagnostic biomarker for LCL-MS as 25 of 45 LCL-MS patients (56%) had anti-AQP4 antibodies but patients who did not have LCL-MS did not have antibodies.

The Mayo Clinic Group has reported that long T2 lesions was a disease marker of NMO[4] but they did not mention spinal cord atrophy, which would also be a marker of NMO. Segmental cord atrophy seems to be caused by severe necrotic lesions in a similar way as long T2 lesions on spinal cord MRI in patients with NMO. The percentage of anti-AQP4 antibodies in patients with segmental long spinal atrophy was not different from that in patients with long T2 lesions, which also supports the hypothesis that the pathomechanism of segmental cord atrophy is similar to that of long T2 lesions.

Similar findings of LCL on spinal cord MRI and seropositivity against AQP4 in NMO and OSMS seem to indicate that these diseases fall into the same clinical spectrum. Some Japanese OSMS patients, however, did not fulfil NMO criteria[4] because they did not have LCL or anti-AQP4 antibodies. Patients with CMS may present with only optic neuritis and myelitis for the first few years after onset, whereas the diagnosis of OSMS requires a 5 year follow-up period after onset.[3] Several patients with OSMS differed from those with NMO, with the disease being clinically restricted to the optic nerves and spinal cord for a period of 5–24 years after the first clinical event. This may be the same clinical phenotype as the benign form of OSMS.[3] All of our patients with OSMS(−) had brain lesions but no brain symptoms or signs. Moreover, they had lower EDSS scores than patients with LCL-MS, indicating that the higher LCL-MS scores may have been caused by LCL.

The role of anti-AQP4 antibody as the primary cause of tissue destruction has not been demonstrated and there were more

Table 2 Relationship between blindness and seropositivity against aquaporin 4 ($p<0.0005$).

	Blindness	
	+	−
Anti-AQP4 antibody		
Positive	7	16
Negative	4	101

relapses in patients with anti-AQP4 antibodies than in seronegative patients. This does not exclude the possibility of a secondary immune response to damage. However, NMO IgG is a known marker of relapse after myelitis with LCL.[12] This suggest that anti-AQP4 antibody/NMO IgG is not the secondary product of tissue destruction, rather it causes necrotic tissue damage and is a marker of a condition related to frequent exacerbation.

Authors' affiliations
Masami Tanaka, Mika Komori, Takahiko Saida, MS Centre, Utano National Hospital, Kyoto, Japan
Keiko Tanaka, Department of Neurology, Brain Research Institute, Niigata University, Niigata, Japan

This work was supported in part by a Neuroimmunological Disease Research Committee grant from the Ministry of Health, Labour and Welfare, Japan.

Competing interests: Researchers from Mayo MS group. Professor Kira, Kyushu University, Japan.

Correspondence to: Dr Masami Tanaka, 8 Ondoyama, Narutaki, Ukyo-ku, Kyoto, 616-8255, Japan; tanaka@unh.hosp.go.jp

Received 5 January 2007
Revised 15 April 2007
Accepted 25 April 2007

REFERENCES

1 **Saida T**, Tashiro K, Itoyama Y, *et al*. Interferon Beta-1b Multiple Sclerosis Study Group of Japan. Interferon beta-1b is effective in Japanese RRMS patients: a randomized, multicenter study. *Neurology* 2005;**64**:621–30.
2 **Okinaka S**, Tsubaki T, Kuroiwa Y, *et al*. Multiple sclerosis and allied diseases in Japan: clinical characteristics. *Neurology* 1958;**8**:756–63.
3 **Misu T**, Fujihara K, Nakashima I, *et al*. Pure optic-spinal form of multiple sclerosis in Japan. *Brain* 2002;**125**:2460–8.
4 **Wingerchuk DM**, Lennon VA, Pittock SJ, *et al*. Revised diagnostic criteria for neuromyelitis optica. *Neurology* 2006;**66**:1485–9.
5 **Pittock SJ**, Lennon VA, Krecke K, *et al*. Brain abnormalities in neuromyelitis optica. *Arch Neurol* 2006;**63**:390–6.
6 **Lennon VA**, Wingerchuk DM, Kryzer TJ, *et al*. A serum autoantibody marker of neuromyelitis optica: distinction from multiple sclerosis. *Lancet* 2004;**364**:2106–12.
7 **Lennon VA**, Kryzer TJ, Pittock SJ, *et al*. IgG marker of optic-spinal multiple sclerosis binds to the aquaporin-4 water channel. *J Exp Med* 2005;**202**:473–7.
8 **Kira J**, Kanai T, Nishimura Y, *et al*. Western versus Asian types of multiple sclerosis: immunogenetically and clinically distinct disorders. *Ann Neurol* 1996;**40**:569–74.
9 **Nakashima I**, Fujihara K, Miyazawa I, *et al*. Clinical and MRI features of Japanese patients with multiple sclerosis positive for NMO-IgG. *J Neurol Neurosurg Psychiatry* 2006;**77**:1073–5.
10 **Tanaka K**, Tani T, Tanaka M, *et al*. Anti-aquaporin 4 antibody in Japanese opticospinal multiple sclerosis. *Mult Scler* in press.
11 **Kurtzke JF**. Rating neurologic impairment in multiple sclerosis: An expected disability status scale (EDSS). *Neurology* 1983;**33**:1444–52.
12 **Weinshenker BG**, Wingerchuk DM, Vukusic S, *et al*. Neuromyelitis optica IgG predicts relapse after longitudinally extensive transverse myelitis. *Ann Neurol* 2006;**59**:566–9.

ELSEVIER

NeuroImage

www.elsevier.com/locate/ynimg
NeuroImage 37 (2007) 1278–1285

Cell-oriented analysis *in vivo* using diffusion tensor imaging for normal-appearing brain tissue in multiple sclerosis

Kenshi Terajima,[a,b,*] Hitoshi Matsuzawa,[a] Keiko Tanaka,[b] Masatoyo Nishizawa,[b] and Tsutomu Nakada[a]

[a]*Center for Integrated Human Brain Science, Brain Research Institute, University of Niigata, Niigata, Japan*
[b]*Department of Neurology, Brain Research Institute, University of Niigata, Niigata, Japan*

Received 20 March 2007; revised 12 June 2007; accepted 26 June 2007
Available online 6 August 2007

There have been several methods proposed so far using diffusion tensor imaging (DTI) for the assessment of normal-appearing brain tissue (NABT) injury in multiple sclerosis (MS). However, for these methods, the analyses of the NABT injury at the cellular level, wherein histological examinations can be used, still present challenging problems. We developed a method of segregating NABT into the following anatomical structures using lambda chart analysis associated with a two-dimensional Gaussian deconvolution of diffusion characteristic functions: 1) structures primarily composed of small neurons and glia; 2) structures primarily composed of large neurons; 3) structures primarily composed of short axons; and 4) structures primarily composed of long axons. Each segregated structure that had a distinctive diffusion characteristic was subjected to the statistical inference of DTI-derived parameters for 14 patients with conventional relapsing–remitting MS (RRMS) and 20 age-matched healthy volunteers. In all of the structures, the trace values were significantly higher and the fractional anisotropy values were significantly lower in the RRMS patients than in the healthy volunteers. Furthermore, the volume fractions of the structures primarily composed of short axons markedly decreased, whereas those of the structures primarily composed of small neurons and glia markedly increased. These results suggest that axonal loss and glial proliferation predominantly occurred in the subcortical white matter and adjacent deep cortical layer, namely, the juxtacortical region. This cell-oriented analysis of NABT injury using DTI confirmed *in vivo* the histological observation that the juxtacortical region is the most vulnerable site in MS.

Introduction

Multiple sclerosis (MS) is a chronic demyelinating disease of the central nervous system with both inflammatory and neurodegenerative processes. Although conventional magnetic resonance (MR) imaging plays an important role in the diagnosis of MS, histological studies have shown that pathological changes are also found in normal-appearing brain tissue (NABT), where conventional MR imaging cannot show abnormal findings (Brownell and Hughes, 1962; Lumsden, 1970; Allen and McKeown, 1979; Kidd et al., 1999; Evangelou et al., 2000; Bjartmar et al., 2001). Furthermore, this NABT injury is considered to be responsible for cognitive or locomotor disability in patients with MS, and has a crucial influence on the prognosis of a patient (De Stefano et al., 1998; Rovaris et al., 1998; Van Buchem et al., 1998; Filippi et al., 1999; Zivadinov et al., 2001; Kalkers et al., 2001; Santos et al., 2002).

A recent advancement in MR technologies enables the analysis of NABT using new imaging techniques. Of these techniques, diffusion tensor imaging (DTI) can provide quantitative information regarding diffusion anisotropy in the central nervous system, and has been increasingly used in various clinical settings. Most of the previous studies using DTI to evaluate NABT injury in MS use either region of interest (ROI) analysis (Werring et al., 1999; Bammer et al., 2000; Filippi et al., 2001; Ciccarelli et al., 2001) or histogram analysis (Van Buchem et al., 1996; Nusbaum et al., 2000; Cercignani et al., 2001a,b) for calculating DTI-derived scalar parameters such as fractional anisotropy (FA) and mean diffusivity (MD). Histogram analysis has now become the standard for NABT analysis in MS, because it is more suitable for the overall assessment of NABT or its principal components, namely, normal-appearing gray/white matter (NAGM/NAWM). Histogram analysis is the best compromise assuming that NABT or NAGM/NAWM cannot be segregated any further into more detailed anatomical structures. However, NAGM/NAWM contains various anatomical cellular components, each of which has a specific diffusion characteristic. NAGM contains relatively large cortical neurons in the cortical surface layer, relatively small cortical neurons in the

* Corresponding author. Department of Neurology, Brain Research Institute, University of Niigata, 1 Asahimachi, Niigata 951-8585, Japan. Fax: +81 25 223 6646.
E-mail address: terajima@bri.niigata-u.ac.jp (K. Terajima).
Available online on ScienceDirect (www.sciencedirect.com).

1053-8119/$ - see front matter © 2007 Elsevier Inc. All rights reserved.
doi:10.1016/j.neuroimage.2007.06.026

cortical deep layer, and glial cells and neurons in the deep gray matter. Similarly, NAWM contains relatively short axons creating short tracts such as U-fibers in the subcortical white matter, and relatively long axons creating long tracts such as corticospinal tracts in the deep white matter. The individual analysis of the pathological changes of these cellular components could be very useful for elucidating the details of the pathogenesis of MS. However, in contrast to histological examinations, such "cell-oriented" analysis of NABT injury using DTI still presents challenging problems.

Recently, a method using DTI for analyzing brain structures showing isotropic diffusion referred to as isotropic component trace analysis has been developed (Matsuzawa et al., 2005). This method using an algorithm for DTI, namely, lambda chart analysis (LCA), enables the segregation of brain structures showing isotropic diffusion into the following anatomical structures having distinct diffusion characteristics: structures primarily composed of small neurons and glia; structures primarily composed of large neurons; and structures mainly containing cerebrospinal fluid (CSF). In this study, we also applied this method to structures showing anisotropic diffusion, which correspond primarily to the white matter. This modified method can effectively segregate NAGM/NAWM into several anatomical structures whose principal cellular components have unique diffusion characteristics. We performed diffusion tensor analyses of these structures in patients with MS and healthy volunteers, and compared the results with previous histological observations.

Subjects and methods

Patients and healthy volunteers

This study was performed in accordance with the human research guidelines of the Internal Review Board of the University of Niigata. Written informed consent was obtained from all the participants. Fourteen patients with MS diagnosed using the 2005 revised McDonald Criteria (Polman et al., 2005), and 20 age-matched healthy volunteers as normal controls were enrolled in the study. The profiles of the subjects are summarized in Table 1. All the MS patients were classified as having conventional remitting–relapsing MS (RRMS) in the remission phase and did not receive steroid therapy at the time of MR data acquisitions. The results of the tests for the anti-aquaporin 4 antibody performed using a method described elsewhere (Tanaka et al., 2007) were negative for the serum samples of all the patients. Six of all the fourteen patients received subcutaneous injection of interferon β-1b (Betaferon®) every other day and the other eight patients received no immunomodulatory therapies, except for intravenous or oral steroid treatment in the relapse phase. All the patients were ambulatory and independent in daily living; they were assessed using the expanded disability status scale (EDSS) (Kurtzke, 1983) less than or equal to 3.5.

Table 1
Profile of participants enrolled in this study

	Control	RRMS
n (F/M)	20 (7/13)	14 (11/3)
Age (range) [years]	33.9±8.8 (19–55)	34.1±12.7 (14–52)
Disease duration (range) [years]		5.1±4.0 (0–12.4)
EDSS (range)		2.6±1.1 (0–3.5)
Brain volume (range) [$\times 10^5$ mm^3]	1.3±0.12 (1.1–1.5)	1.2±0.09 (1.1–1.4)
Lesion volume (range) [$\times 10^3$ mm^3]		3.1±3.3 (0–8.8)
Volume fraction of lesion (range)		0.025±0.026 (0–0.073)

Values (excluding those in the first row) are expressed as mean±standard deviation, with their ranges in parentheses.
RRMS=relapsing–remitting multiple sclerosis.
EDSS=Expanded Disability Status Scale.
Volume fraction of lesion=volume fraction of multiple sclerosis lesion to whole brain of slice.

Data acquisition

A General Electric (Waukesha, WI, USA) Signa 3.0T system was used to perform all MR studies. Four contiguous slices of diffusion-weighted images were obtained using spin-echo echo-planar sequences with the following parameter settings: field of view (FOV), 20 cm × 20 cm; matrix, 128 × 128; slice thickness, 5 mm with a 2.5 mm interslice gap; repetition time (TR), 2000 ms; echo time (TE), 82.7 ms; and number of acquisitions (NEX), 8. The *b*-value was 1000 s/mm^2 for each axis with the six combinations of diffusion gradient vectors as follows: (1, 0, 1), (−1, 0, 1), (0, 1, 1), (0, 1, −1), (1, 1, 0), and (−1, 1, 0), where the (*x*, *y*, *z*) directions correspond to (read-out, phase, slice), respectively. Structural images were also obtained using a fast spin-echo sequence.

Data analysis

The obtained MR data were analyzed as follows using *EZ-LCA* scripts and in-house routines written in MATLAB (MathWorks, Natick, MA, USA). *EZ-LCA* is available at http://coe.bri.niigata-u.ac.jp/.

Diffusion tensor analysis and lambda chart analysis

The slice of interest was selected at the level of the body of the lateral ventricle. Visible plaques in the RRMS patients were identified to measure their volume, using semiautomated in-house routines by referring to their corresponding structural fast spin-echo images, and were excluded from the following analyses. First, diffusion tensor analyses of all of the pixels were performed and two parameters, lambda longitudinal (λ_L) and lambda transverse (λ_T), were calculated as follows:

$$\lambda_L = \lambda_1,$$
$$\lambda_T = \frac{\lambda_2 + \lambda_3}{2},$$

where λ_1, λ_2, and λ_3 are the three eigenvalues of the apparent diffusion tensor in descending order. Subsequently, the λ_L values of the pixels were plotted against the λ_T values, creating a two-dimensional chart, namely, a lambda chart (Fig. 1A). Any given pixel (λ_T,λ_L) on the chart can also be treated in the polar coordinates. The anisotropic angle θ is directly obtained from the polar angle in the polar coordinates, or using the equation $\theta = \arctan(\lambda_L/\lambda_T)$. Therefore, the diagonal line $\lambda_L - \lambda_T = 0$ or $\theta = \pi/4$ represents the isotropic line (blue line on the chart), indicating isotropic diffusion. As θ increases, diffusion anisotropy increases. The trace (Tr) of the apparent diffusion tensor is determined as

$$\mathrm{Tr} = \lambda_1 + \lambda_2 + \lambda_3 = \lambda_L + 2\lambda_T \text{ or } \mathrm{Tr} = r(\sin\theta + 2\cos\theta),$$

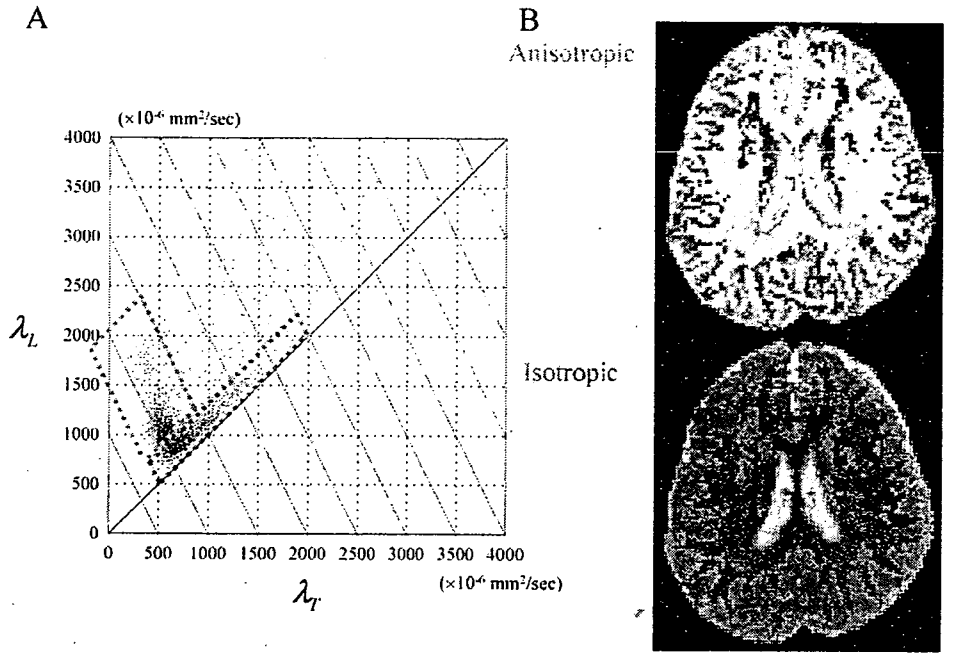

Fig. 1. Lambda chart analysis. (A) Diffusion tensor analyses of all pixels on the slice of interest were performed and the two parameters $\lambda_L=\lambda_1$ and $\lambda_T=(\lambda_2+\lambda_3)/2$ were calculated, where λ_1, λ_2, and λ_3 are the three eigenvalues of the apparent diffusion tensor in descending order. The scatter plot of the chart clearly shows that there is an L-shaped cluster of pixels with the right-side arm along the blue isotropic line (the deep sky blue-dotted area) and the left-side arm parallel to the red isotrace lines (the dark orange-dotted area). The right-side arm corresponds to the group of pixels showing isotropic diffusion, and the left-side arm corresponds to the group of pixels showing anisotropic diffusion. (B) The pixel position on the chart is determined solely by the diffusion characteristics of each pixel and is totally independent of the corresponding information regarding the position on the image matrix. By remapping the pixels of each arm of the cluster back onto the original image matrix, it is apparent that the right-side arm primarily represents the gray matter, as shown by the deep sky blue pixels, whereas the left-side arm primarily represents the white matter, as shown by the dark orange pixels.

where r is the radius in the polar coordinates. Isotrace lines (red lines that cross the isotropic line on the chart) are, therefore, given by the equation $\lambda_L+2\lambda_T=\mathrm{Tr}$ for a fixed Tr.

It becomes immediately apparent that there is an L-shaped cluster of pixels. The right-side arm of the cluster along the isotropic line corresponds to the group of pixels showing isotropic diffusion, and the left-side arm of the cluster parallel to the isotrace lines corresponds to the group of pixels showing anisotropic diffusion (Fig. 1A). The pixel position on the lambda chart is determined solely by the diffusion characteristics of each pixel and is totally independent of the corresponding information regarding the position on the image matrix. By remapping the pixels of each arm of the cluster back onto the original image matrix, it is apparent that the group of pixels showing isotropic diffusion primarily represents the gray matter, whereas the group of pixels showing anisotropic diffusion primarily represents the white matter (Fig. 1B). The details of the lambda chart analysis can be found elsewhere (Matsuzawa and Nakada, 2000).

Two-dimensional Gaussian deconvolution

By considering the results shown in Fig. 1, further partitioning of the pixels on the lambda chart is expected to provide more detailed anatomical segmentation of the brain structure. In this study, parallelogram compartments were used for the partitioning, as shown in Fig. 2. Each parallelogram compartment is surrounded by two pairs of parallel lines. The lines of one of the pairs are parallel to the isotrace lines and are given by the equation $\lambda_L+2\lambda_T=$constant. The lines of the other pair are parallel to the isotropic line and are given by the equation $\lambda_L-\lambda_T=$constant. Therefore, the ranges of the two parameters, namely, $\mathrm{Tr}=\lambda_L+2\lambda_T$ and $\Delta\lambda=\lambda_L-\lambda_T$, determine the parallelogram compartment on the lambda chart.

Here, we adopted the nonorthogonal coordinate system of Tr versus $\Delta\lambda$ to analyze the distributions of these two parameters. All the pixels on the lambda chart created a Tr function when plotted against their Tr. On the other hand, the pixels also created a $\Delta\lambda$ function when plotted against their $\Delta\lambda$.

Subsequently, the Tr function was deconvolved into five Gaussian elements, and the $\Delta\lambda$ function into three Gaussian elements, both of which were performed by curve-fitting processes using a multiple Gaussian mixture model (Fig. 2). Initially, the first Gaussian curve in the mixture model to fit to the Tr or $\Delta\lambda$ function was estimated by a chi-square process. Then, the second Gaussian curve to fit to the residual data was also estimated by a chi-square process. The processes were repeated until all the Gaussian curves in the model were estimated. Subsequently, the nonlinear least-squares formulation to fit the Gaussian mixture model was determined using the trust-region algorithm implemented in the MATLAB Curve Fitting Toolbox, with the coefficient constraints specified in the chi-square processes described above. These curve-fitting processes were completely automatic across all the subjects including the healthy volunteers and RRMS patients.

The number of Gaussian elements in the current analyses was five in the Tr function in spite of its continuous distribution up to Tr values higher than the values that these five Gaussian elements cover. However, the first five Gaussian elements gave sufficient ranges of the Tr values for segregating NABT excluding CSF in the